

Exudates Detection in Diabetic Retinopathy by Two Different Image Processing Techniques

Sara S. Aldeeb, Selçuk Sevgen

Department of Computer Engineering, Istanbul University School of Engineering, İstanbul, Turkey

Cite this article as: S.S. Aldeeb, "Exudates Detection in Diabetic Retinopathy by Two Different Image Processing Techniques", *Electrica*, vol. 18, no: 2, pp. 177-186, 2018.

ABSTRACT

Different techniques developed in the previous decades are used for blood vessel detection. Different kinds of image processing approaches in the detection and analysis of blood vessels can be applied to diagnose many human diseases and help in various medical and health diagnoses. Image processing for blood vessels could be used in areas such as disease diagnosis, severity measurement of specific diseases, and in biometric security. This study compares two different techniques to accurately diagnose a specific disease according to some selective features. Diabetic retinopathy is used for this comparative study as it is one of the most severe eye disorders and chronic diseases to cause blindness. Classifications and accurate measurements for blood vessel abnormalities (exudates, hemorrhages, and micro-aneurysms) enabled the correct and accurate diagnosis in retina and diabetic retinopathy. To avoid blindness, it is essential to utilize fundus image processing application to facilitate the early discovery of a diseased retina. Throughout the fundus automated image process, the retinal features are extracted. The techniques applied in this study are a morphological-based image processing technique and an edge detection technique using Kirsch's template. First, the application of these image processing techniques are described and explained in detail. Subsequently, a classification process is proposed to assess and evaluate the performance of each technique.

Keywords: Diabetic retinopathy, optic disc, exudates, morphology, Kirsch's template

Introduction

Blood vessel assessment and segmentation play a key role in the diagnosis of many different kinds of diseases such as retinal disorders in diabetic retinopathy, macular degeneration, and glaucoma that may cause a gradual loss of eyesight and could be a reason for blindness. The manual detection of narrow blood vessels on retinal images is time-consuming and may result in erroneous output. Hence, automated systems, computer aided, robust performance-oriented algorithms are all required to detect and segment the blood vessels and diagnose their associated diseases efficiently.

Segmentation, detection, and measuring the diameter of retinal blood vessels are essential for an accurate diagnosis and precise treatment of many ocular diseases such as diabetic retinopathy (DR) [1].

Diabetic retinopathy was selected for the purpose of this study. By applying an automated algorithm from an obtained retinal fundus image it could be classified as healthy (normal) or unhealthy (suffers from DR). DR is categorized as one of the most severe eye diseases worldwide. The symptoms could badly affect the vision of patients and could be escalated to reach blindness in some cases if neglected.

Diabetic retinopathy is identified and characterized by the growth of retinal microaneurysms, hemorrhages, and exudates which are all main aspects to be tracked during a DR diagnosis.

The more micro-aneurysms, hemorrhages, and exudates in number, the more severe the disease is [2-4]. Exudate detection was the main focus of this study since it is a significant sign of

Corresponding Author:

Selçuk Sevgen

E-mail:

sevgen@istanbul.edu.tr

Received: 29.12.2017

Accepted: 18.03.2018

© Copyright 2018 by *Electrica*

Available online at

<http://electrica.istanbul.edu.tr>

DOI: 10.5152/ijueee.2018.1822

diabetic retinopathy and an indication of the co-existence with retinal edema. Vision could be lost in case of exudate expansion into the macular area.

In the traditional method of DR diagnosis, the patient's pupil is dilated using the chemical, Tropicamide 1%, which could cause side-effects in some patients. It is a time-consuming, inconvenient method of diagnosis for ophthalmologists [5].

Recently, some automated image processing techniques have been developed and applied to retinal images for exudate detection and analysis as a substitution for the traditional diagnostic method.

In the study of Sinthanayothin et al. [6] the RRGs algorithm was applied. The basis of RRGs depends on the identification of similar pixels within a certain region so that the boundary location could be determined. The adjacent pixels of the same regions tend to have homogeneous gray-level characteristics.

Usher et al. [7] applied an adaptive intensity thresholding beside RRGs for detecting exudate areas. After extracting the candidate regions, they were used as input to an artificial neural network. By applying the RRGs algorithm, the separation results of dark and bright lesions were affected by the poor-quality images using exudate feature extraction and thresholding. Gardner et al. [8] applied an artificial neural network technique to propose an automated detection for diabetic retinopathy.

Mainly the candidate exudate regions are recognized from the gray-level images. Back-propagation neural network was primarily used for analyzing the retinal fundus images but this technique was not reliable enough for the low contrast images. Thus, RRGs and thresholding techniques are more widely applied in this study area.

Liu et al. [9] presented an automated exudate detection technique that used a *region-growing* and thresholding algorithm where the optic disc and fovea were identified using Hough transform and blood vessels that were traced by a Gaussian filter. Osareh et al. [10] used fuzzy C-means clustering that followed some preprocessing steps. From a colored retinal image, it classified the segmented regions into exudative and non-exudative areas. Also, an artificial neural network classifier was investigated. On the LUV color space, the system performance is good despite the *low level* of detection accuracy in the non-uniform illumination case. Mitra et al. [11] used the Naïve Bayes classifier to diagnose diabetic retinopathy from the retinal fundus image. The performed system could help ophthalmologists as a tool of decision support. For this proposed automated diagnosis of the disease, two different fundamental image processing approaches have been applied. The first technique is using Morphological operators and the second is applying Edge detection using Kirsch's template. The final resulting images from the previously applied techniques were passed through a classification phase.

Materials and Method

All retinal images used in this study were digital and belong to non-dilated pupils from diabetic retinopathy patients. The images used for testing purposes are taken from the DIARETDB1 v2.1 and STARE database [12, 13]. They are both public datasets and mainly used as a point of reference for detecting diabetic retinopathy. Figure 1 represents an example of a retinal fundus image which includes exudates and some other retinal components such as microaneurysms, the optic disc, etc.

Methods used and applied in this study depend on two major image processing techniques: Morphological Technique and Edge Detection Technique using Kirsch's template. The final output from both algorithms are shown and a comparative analysis will be illustrated showing which technique achieved higher performance rates and the reason behind each. The classifiers used for evaluating each technique are, the Support Vector Machine (SVM) and the Naïve Bayes (NB). Prior to this classification phase some features were extracted as well.

Morphological Technique

The Morphological technique uses operators such as closing, opening, erosion, and dilation. This technique includes three stages: preprocessing, optic disc elimination, and exudate detection.

The pre-processing stage can be regarded as the foundation of this work as shown in Figure 2. The main goal of pre-processing is minimizing the *noise* effect, *contrast enhancement*, and refining the inconsistent illumination. Pre-processing includes RGB conversion to HSI followed by a median filter to reduce noise. The resulting image is submitted to CLAHE to enhance the contrast of small regions [14]. Contrast enhancement assigns high-intensity values of the optic-disc and exudates that are usually shown in the I-band of the same objects [5-6].

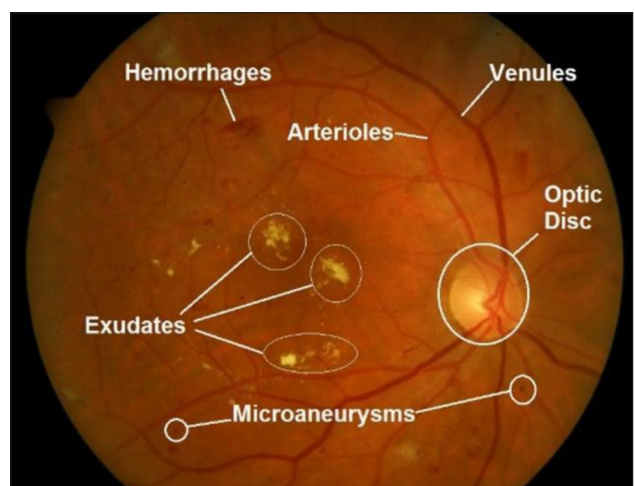


Figure 1. Full retinal image includes Optic Disc, Exudates, Micro-aneurysms, and Hemorrhages.

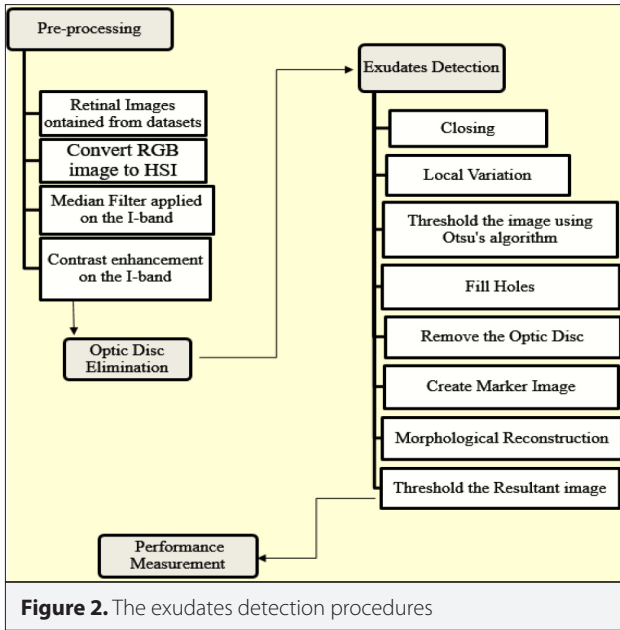


Figure 2. The exudates detection procedures

Optic Disc Elimination

The optic disc should be removed prior to the exudate detection, as it appears similar in intensity; color, and contrast to the exudates on the retinal image [5, 15-18].

Although blood vessels appear with a high contrast, the optic disc is distinguished by the largest circular area with the same high contrast compared with the nearby smaller areas that represent blood vessels. To eliminate the remaining blood vessels inside the optic disc a morphological closing operator (φ) has been applied with a structuring element (Se_1) that is shaped as a flat disc. The result after applying the closing operator is shown in Figure 3 a, and Equation (1) and was applied in [15].

$$OD_1 = \varphi(Se_1)(OI) \quad (1)$$

where OI is the original fundus image. A threshold (α_1) was applied to the resulting image as shown in Figure 3 b. The resultant bi-image was used as a mask. To remove the candidate bright regions, the whole obtained pixels from the previously applied mask were inverted and then overlaid on the original image. Figure 3 c, shows the result in OD_2 . A morphological dilation D was then applied after that to the overlaid image.

$$OD_3(x) = D_{OI}(OD_2) \quad (2)$$

A repeatable morphological dilation was applied to the marker image (OD_2) and under the mask image (OI) until both of the contours fit together. The resultant reconstructed image is shown in Figure 3 d. The difference between the original image (OI) and the dilated image (reconstructed) (OD_3) is thresholded at a gray level α_2 as illustrated in the next equation.

$$OD_4 = T_{\alpha_2}(OI - OD_3) \quad (3)$$

Note that, the value of α_2 is not fixed and varies according to the automated selection while applying Otsu algorithm. As shown in Figure 3 e, areas with high intensity are reconstructed while others are eliminated. The optic disc in normal cases can be identified and recognized as the greatest bulk among the other areas. Sometimes in cases of severe exudates and advanced DR, some areas may appear larger than the optic disc. Due to the roundness of the shape of the optic disc, the selection process for the optic disc is specified by the largest shape among other regions that also have a circular structure. The circularity of a certain shape is computed and identified by the value of compactness, CP , as illustrated using the following equation.

$$CP = 4\pi \frac{area}{Perimeter^2} \quad (4)$$

where the area is the whole number of pixels that form a certain shape and the perimeter is the total number of pixels that belong to the surrounding line or border of a shape. A binary dilation was applied to the resulting largest circular shape OD_5 among others using a binary dilation operator (δ) in Equation (5). At this step, a flat disk-shape (Se_2) is used to ensure that all pixels belong to the optic disc are mostly covered.

$$OD_{fin} = \delta(Se_2)(OD_5) \quad (5)$$

Figure 3 f, shows that the whole optic disc is masked out in the original image. Then, the optic disc was masked out from the original image so that the final result could be shown as Figure 3 g. The final result from the optic disc detection and elimination phase was inverted with black-white inversion. Hence, this last output will be the main input image to be used for *Exudate Detection* in the following phase. Figure 3 h, represents the final result of the optic disc detection and elimination phase.

Exudate detection

By using a closing operator, high contrast vessels can be removed similar to the previously performed steps. The result from this dilation is demonstrated in Equation (6) as $E1$ and is shown in Figure 4 a. To show exudates inside the retinal image with all of their main characteristics clustered in a close distribution form, a local variation operator is applied and the resulting image, $E2$, is shown in Figure 4 b [15].

$$E_2(x) = \frac{1}{N-1} \sum_{i \in W(x)}^n (E_1(i) - \mu E_1(x))^2 \quad (6)$$

Using the Otsu algorithm, the previous result was automatically thresholded at the gray level α_3 to erase the regions of low-local variation. Using a flat disc structure element (Se_3) a binary dilation was applied to make sure that all the neighboring pixels of the thresholded result are also included in the candidate regions. Equation (7) indicates the previous process. Figure 4 c, shows the result.

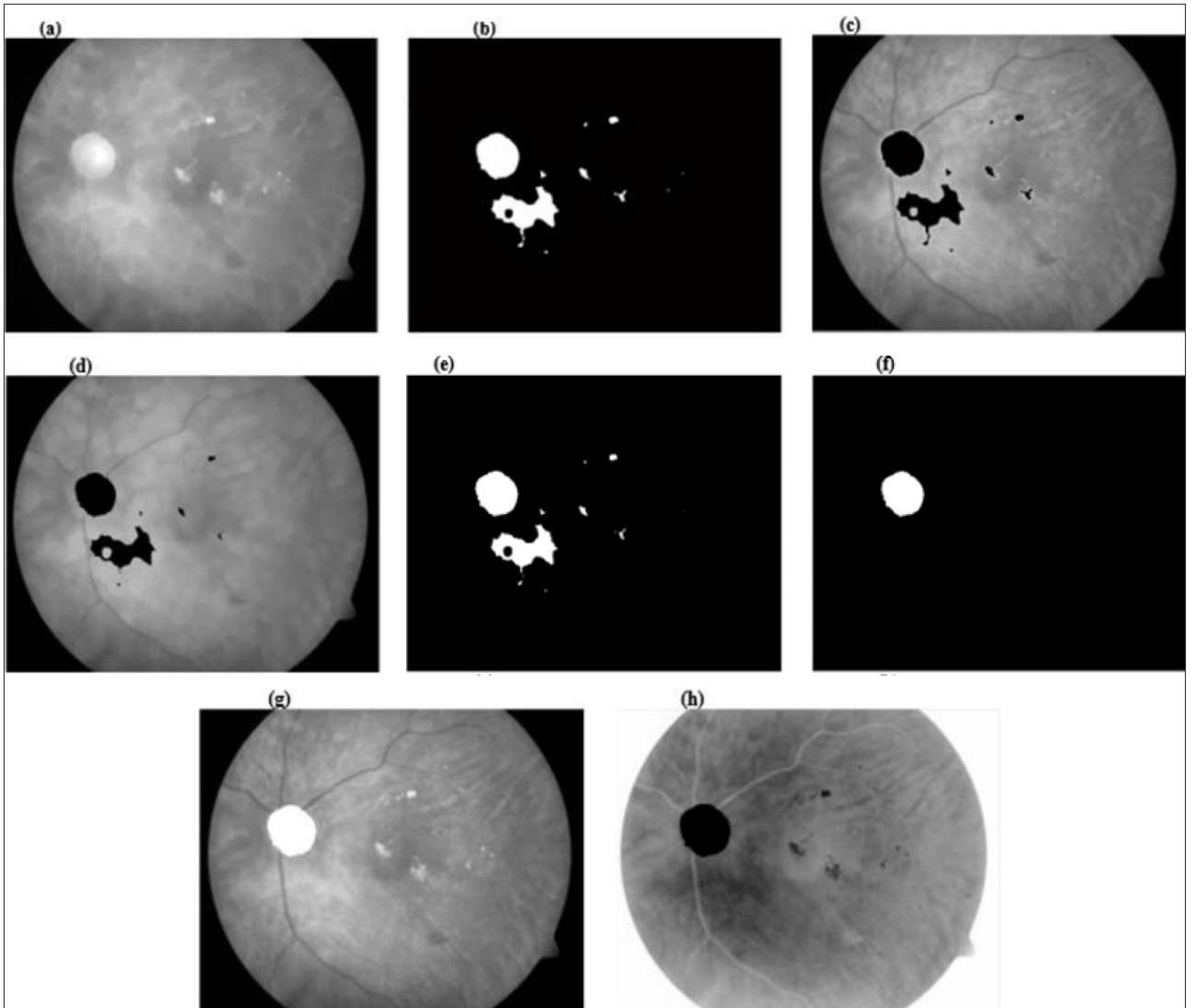


Figure 3. Optic Disc detection and elimination. Morphological closing on I-band image(a); Thresholded image (binary conversion) (b); Marker image (c); Dilation of the marker image (d); Final image after thresholding (e); Biggest blob selection (f); Elimination of Optic disc from the enhanced contrast image(g); Inverted BW after eliminating OD from the retinal image (h)

$$E_3 = \delta(Se_3) (T_{\alpha 3} (E_2)) \quad (7)$$

Some of the previously detected candidate regions contain holes inside them. To have these regions in a solid block form, a flood-filling technique was applied. (E_4) represents this image and the result is shown in Figure 4 d. Prior to OD elimination from the previous resulting image (E_4), a binary morphological dilation was applied to the final result from OD elimination. (OD_{fin}) using a flat disc structure element (Se_4), Equation (8) illustrates this processing and the result E_5 is shown in Figure 4 e,

$$E_5 = E_4 - \delta(Se_4) (OD_{fin}) \quad (8)$$

The result E_5 is then used as a mask and a marker image is created in E_6 and shown in Figure 4(f). Similarly, as shown in the

previous steps, a morphological reconstruction has been performed on E_6 and the result E_7 is displayed in Figure 4 g.

The difference between the original image (OI) and the reconstructed image (E_7) is thresholded using a constant gray level α_4 . The final obtained image is (E_{fin}) and mathematically illustrated by Equation (9). Figure 4 h, shows the final obtained image that includes only the detection exudates from a retinal fundus image.

$$E_{fin} = T_{\alpha 4} (OI - E_7) \quad (9)$$

Edge Detection Technique Using Kirsch's Template

One of the major keys for the identification of exudates, the optic disc, and blood vessels in the retinal fundus image is IM-

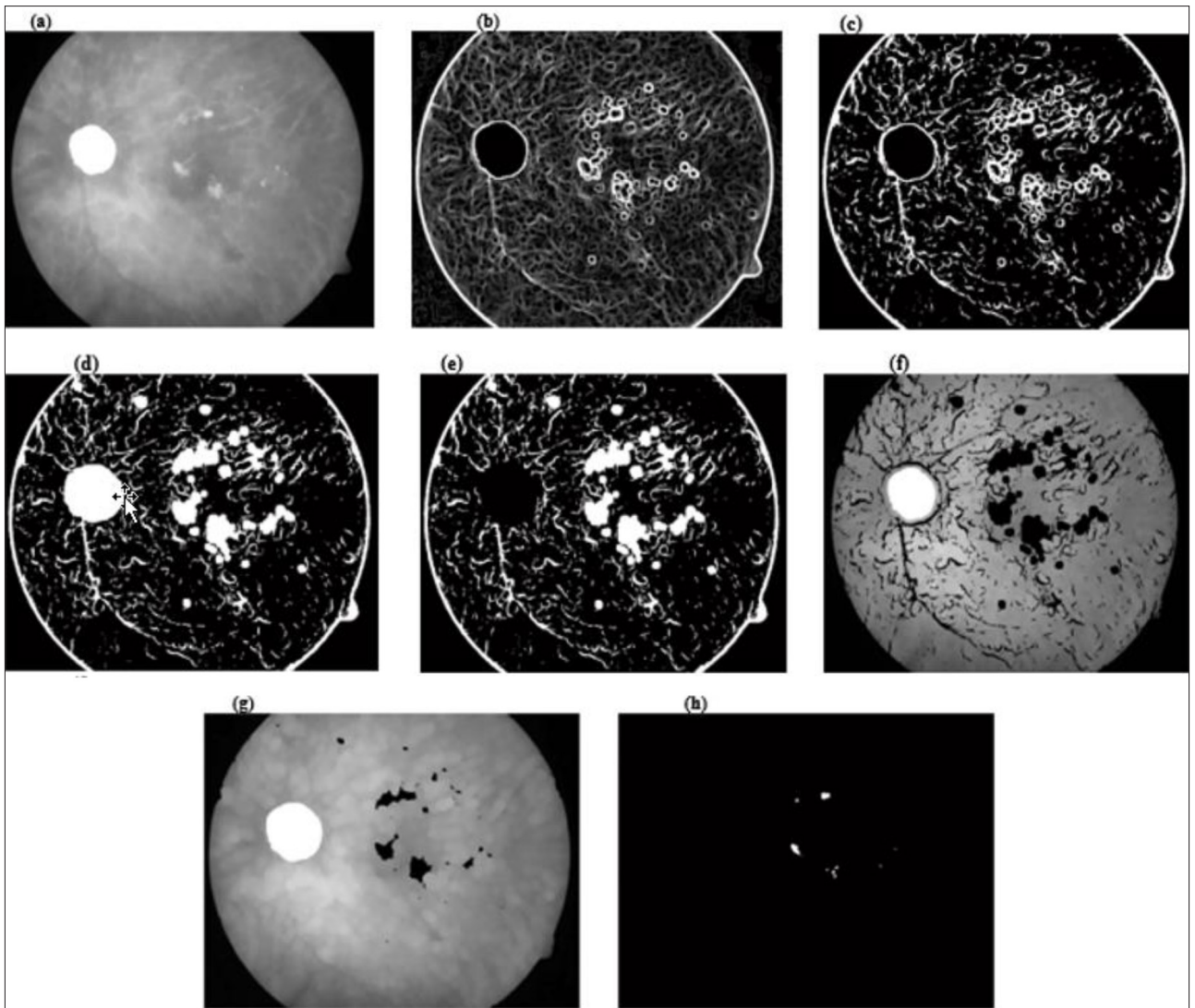


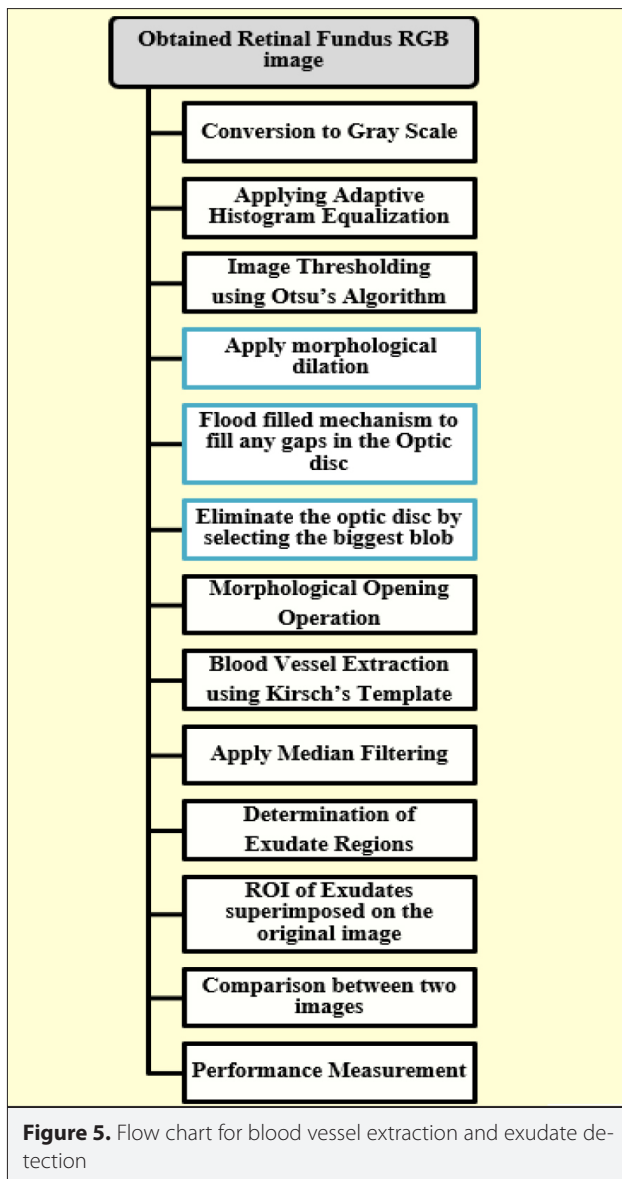
Figure 4. Exudates detection Blood Vessels eliminated by closing (a); Image from local variation(b); Thresholded image (binary conversion) (c); Applying flood-filling on enclosed areas(d); Removing the optic disc (e); Marker image(f); Image dilation (reconstructed) (g); Detected exudates from the final image (h)

AGE SEGMENTATION and edge detection is a part of this image segmentation [19].

Kirsch's template is one of the fundamental approaches in edge detection and here it is used for blood vessel detection from the obtained retinal images. Out of several templates, it tends to find the maximum edge strength in a few present directions [20]. Similar to the preprocessing committed before in the first discussed technique, the obtained retinal images from a dataset are subjected to a pre-processing stage in order to prepare them for the core process. After preprocessing with three different algorithms; *Edge detection*, *Otsu thresholding* and *Morphological Operations* are then applied for an efficient extraction of the retinal exudates and the optic disc regions. The proposed algorithm is schematically designed in Figure 5 for exudate detection using the Kirsch's template.

The original colored image in RGB color space was acquired from the selected datasets and is shown in Figure 6 a. First, the RGB image is converted into grayscale shown in Figure 6 b. Then, a contrast enhancement is committed on the previously obtained grayscale image using *Adaptive Histogram Equalization (AHE)* as shown in Figure 6 c. This algorithm uses contrast enhancement limits, namely 'clipLimit' as 0.001 [21].

The resulting image is then binarized by selecting an appropriate threshold level using *Otsu's algorithm* shown in Figure 6 d. This step helps in detecting the hard exudates from the contrast enhanced retinal fundus image. A binary dilation has been applied on the thresholded image using a flat disk-shaped structuring element as shown in Figure 6 e. The previously detected areas are flood-filled to fill all gaps inside the optic disc so it can be shown as a solid compact as in Figure 6 f. The optic



disc will be eliminated by *selecting* the biggest blob algorithm that was previously applied, with the result shown in Figure 6 g. The same contrast enhanced retinal fundus image has then undergone a binary opening operator as shown in Figure 6 h. A morphological opening is applied using disk-shaped structuring elements to enhance the *blood vessel and exudate* edges. The previous result is then subjected to Kirsch's template for *blood vessel and exudates* extraction, as shown in Figure 6 i. For edge detection, the operator uses eight templates, which are successively rotated by 45 degrees [20]. Thereafter, a median filter is applied on the image to reduce the effect of salt and pepper noise and the resulting image is shown in Figure 6 j.

Then, the filtered image with the extracted *blood vessels and exudates* is subtracted from the binarized image (obtained using Otsu's algorithm) to locate the regions where exudates *only* have

been formed as shown in Figure 6 k. The resulting image contains both exudates and the optic disc. For that reason, an extra enhancement step was performed to get a final output image with only the detected exudates. A second subtraction from the resulting image for the result of the biggest blob is done so the final obtained output image from this technique is a binary image with only the retinal detected exudates shown in Figure 6 k.

In the literature, previously completed experiments and studies using Kirsch's template were used for detection of both exudates and OD. No optic disc elimination process was applied in the final obtained result shown in Figure 6 l. In other words, all processes related to OD elimination were recently added to this algorithm as a part of its enhancements. Thus, the final examined binary image contains only the detected exudates.

Finally, the performance parameters are measured to evaluate the efficiency of the proposed algorithm.

Results

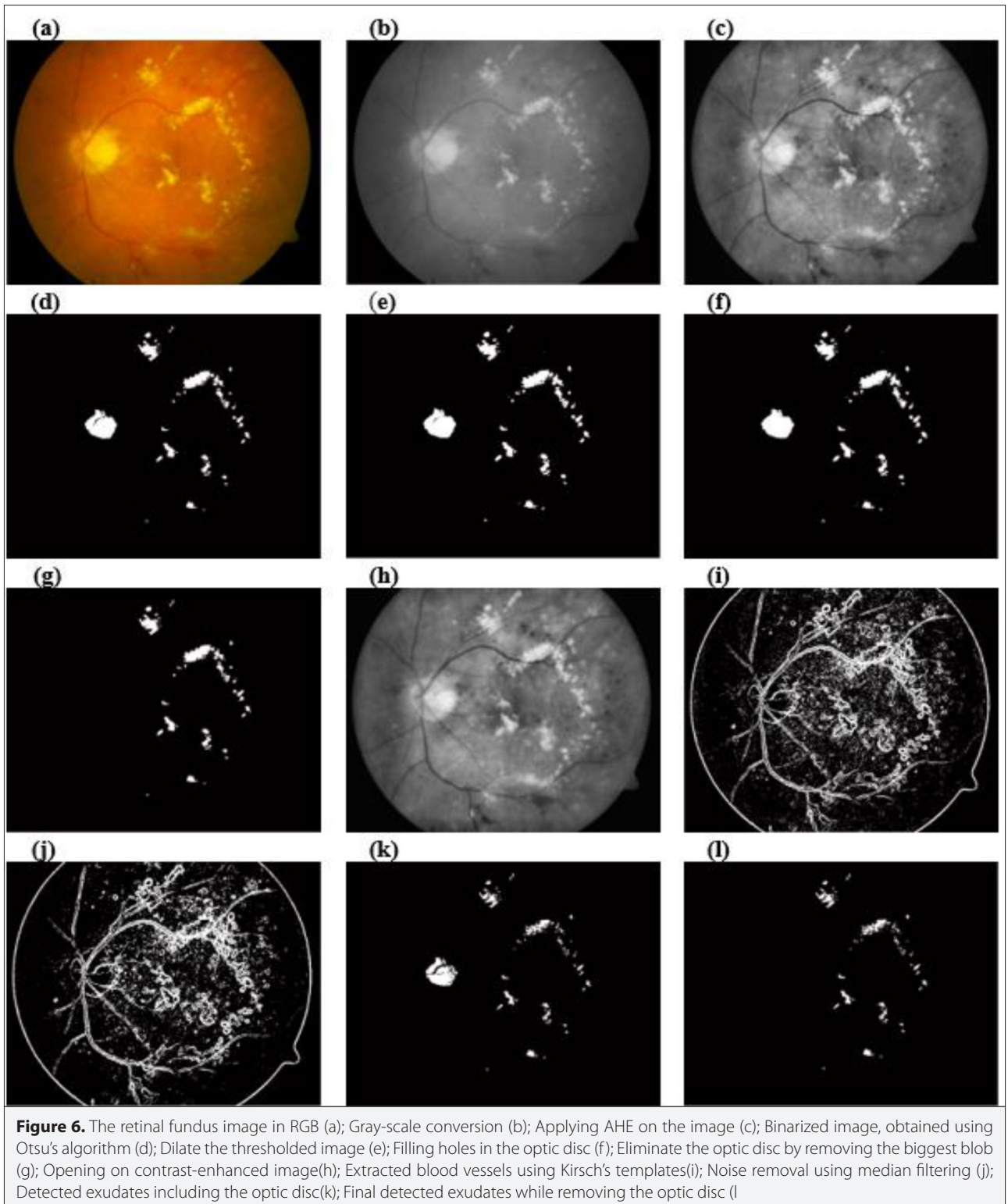
In this study, fifty images were tested on a Lenovo idea pad 700 Intel Core i7 6700HQ 2.60 Hz. / 2.59 GHz 16 GB notebook computer using MATLAB. The total processing time taken for each image was approximately 10.63 sec. (considering the elimination of the optic disc that took around 5.32 seconds) while applying the first morphological technique. However, the processing time for each image was 9.25 seconds obtained from Kirsch's templates.

Accuracy (Acc.), Recall/ sensitivity (Rec.), and Precision (PPR) criteria were chosen for performance measurement of the previously applied techniques in in this study. Classification algorithms are used to calculate these criteria. Two different classification algorithms have been chosen for that purpose:

- Support Vector Machine
- Naive Bayes

Feature extraction is a retrieval characteristic of an object image which is a unique value differentiator to compare with another object. It has been found that there are many features, *around 18* [22], including color, shape, texture, area, and perimeter, etc. These features should be considered in the retinal image while detecting diabetic retinopathy. Finally, among all of these features, three are empirically selected as they reflect the best characteristics that ophthalmologists depend on through their primary diagnosis according to many medical sources and literature reviews for this phase; which are *area, perimeter, and number of white pixels* as they were the most obvious features found in the binary images. These group of selected features achieved relatively high rates of accuracy and the lowest misclassification.

First, a literary survey using illustration tables has been done to show a comparative study on various performance parameters of the previously proposed techniques as shown in Table 1 and Table 2.



From the previously obtained numerical results of the performance measurements and the visual results of both techniques, Morphological algorithm and Kirsch's template algorithms, three different criteria explain which technique is more reliable in practice. They are as follows:

Time

Kirsch's template algorithms processing time was 9.25 seconds while Morphological operator algorithm processing time was 10.63 seconds. That means in terms of time that Kirsch's template

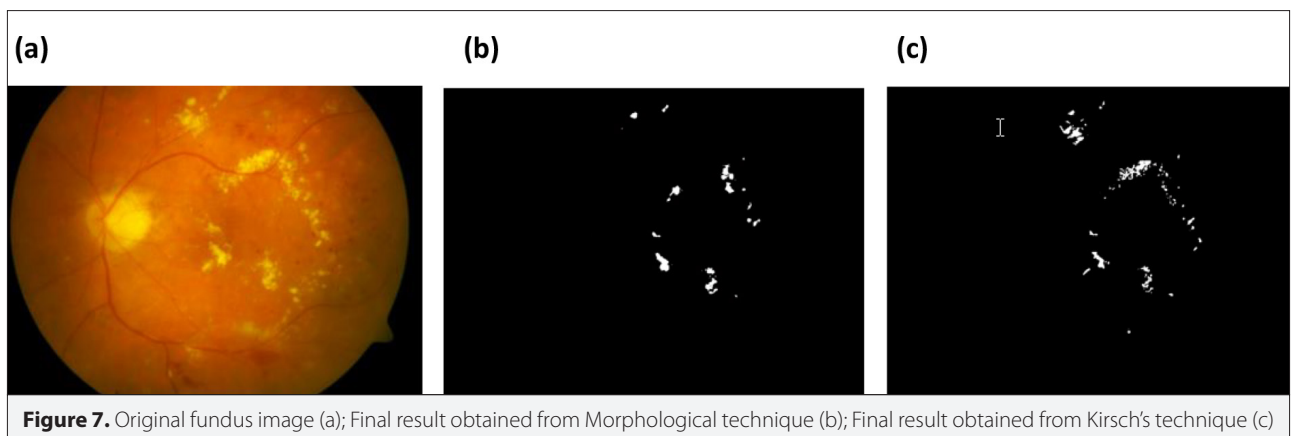


Figure 7. Original fundus image (a); Final result obtained from Morphological technique (b); Final result obtained from Kirsch's technique (c)

Table 1. Accuracy, Recall and Precision % for both techniques using SVM classifier

Technique	Acc.	Rec.	PPR	Mis. Portion
Morphological Technique	%96.66	%96.7	%96.9	%3.33
Kirsch's templates technique	%96.875	%96.9	%97.1	%3.125

Table 2. Accuracy, Recall and Precision % for both techniques using NB classifier

Technique	Acc.	Rec.	PPR	Mis. Portion
Morphological Technique	%96.66	%96.7	%96.9	%3.33
Kirsch's templates technique	%100	%100	%100	%0

techniques achieve higher time-saving rates despite the slight difference between both processing time durations per one image.

Preciseness

After examining the final visual results (binary image) from both techniques by an ophthalmologist, we are convinced that Kirsch's template technique are more precise and accurate in its final result for the shapes and detected texture of the exudates than the Morphological technique as shown in Figure 7.

Efficiency

According to the performance measurements resulting from the selected classifiers, Kirsch's template techniques gains over the Morphological techniques with its higher rates of accuracy, recall, and precision with both classifiers SVM and NB as illustrated in Table 1, 2.

The optic disc and exudates both have similar intensity characteristics, therefore, optic disc detection and elimination was performed before the exudate detection commenced. Around fifty non-dilated fundus retinal images with relatively high rates of accuracy, recall and low misclassification portion produce a guaranteed and trusted automated system for the diagnosis of DR.

The ophthalmologist's workload could be minimized while using this system for disease detection. It could provide an early and fast diagnosis of DR especially if there are few available ophthalmologists in an area. These techniques and automated system will help ophthalmologists significantly with a fast and easy detection of DR symptoms throughout the screening process. Hence, it is a more reliable method for diagnosis. According to the demonstrated results given here, the DR automated detection system could be very effective in detecting exudates based on the intensity of retinal fundus images.

However, human intervention and ophthalmologists help are still required for some few cases where the identified results are not clear enough.

Conclusion

This study presents professional detection of the optic disc in retinal fundus images while considering the similar intensity of both exudates and the optic disc (high-intensity areas). Thus, the optic disc is eliminated before exudate detection to avoid contradiction. It also detects the existing retinal exudates, measures the amount of these exudates by the number of pixels displayed in white color inside the binarized processed image, and lastly calculates its area and perimeter.

This automated detection system can precisely diagnose the existence of DR so that there is no need to apply any chemicals to dilate the retina and cause patients pain. Thus, it decreases the human interference in the process of disease diagnosis to its lowest level. However, in some cases, additional diagnosis is still needed. This automated system depends on non-dilated retinal fundus digital images instead of the classical analysis used for DR diagnosis which mainly relies on dilating

the patient's pupil by chemicals. Hence, it could be helpful in two ways. First, it avoids the use of chemicals that may cause side-effects and hurt the patient and second, it saves time for the ophthalmologists.

There are some factors that would affect the detection abilities of this automated system and the final output such as; low-quality retinal images, no unified degree of intensity due to poor capturing equipment for the fundus images, the existence of very faint retinal exudates or exudates that are so close to blood vessels that they would be misclassified as normal (no existence for DR), and the existence of high contrasted choroidal blood vessels that may be detected as exudates even when using closing operators to reduce high contrast. All of these factors could affect the sensitivity of the automated system and lead to a lower DR detection rate.

In the future, it is intended to expand and improve the detection ability of the automated DR system to include localized micro-aneurysms, hemorrhages, and measuring the degree of severity of DR.

Furthermore, multi-classification is intended as a proposal for future work in which to measure and determine the DR degree of severity. Thus, the diagnosis system from the obtained retinal image will not only determine the existence of DR but will also define the degree of DR severity the patient has. Basically, there are three stages of DR severity: Normal, Moderate NPDR, and Severe NPDR. For the future, updating the previously discussed techniques to be able to diagnose the DR's stage, blood vessels and hemorrhages detection will be considered beside exudate detection. Additional features will be added to the previously discussed three features for a complete, accurate, and efficient classification and system evaluation. These are the perimeter and the area of both hemorrhages and blood vessels at each of R, G, and B color components. Present ranges used by ophthalmologists for the input values of area and perimeter of both blood vessels and hemorrhages determine at which stage the diabetic retinopathy patient is.

Peer-review: Externally peer-reviewed.

Conflict of Interest: The authors have no conflicts of interest to declare.

Financial Disclosure: The authors declared that this study has received no financial support.

References

1. T. Chanwimaluang, G. Fan, "An efficient blood vessel detection algorithm for retinal images using local entropy thresholding in Circuits and Systems", ISCAS'03. Proceedings of the 2003 International Symposium on IEEE, 2003.
2. M. Humayun, H. Lewis, H. W. Flynn, P. Sternberg, M. S. Blumenkranz, "Management of submacular hemorrhage associated with retinal arterial macroaneurysms", *Am J Ophthalmol*, vol. 126, no. 3, pp. 358-36, 1998.
3. J. Kanski, "Diabetic retinopathy, clinical ophthalmology", Oxford: Butterworth-Heimann, 1997.
4. P. G. Swann, "Non-retinal ocular changes in diabetes", *Clin Exp Optom*, vol. 82, no. 2-3, pp. 43-46, 1999.
5. M. Niemeijer, B. Van Ginneken, Staal, J. Stall, M. S. Suttorp-Schulten, M. D. Abràmoff, "Automatic detection of red lesions in digital color fundus photographs." *IEEE Trans on Med Imaging*, vol. 24, no. 5, pp. 584-592, 2005.
6. C. Sinthanayothin, J. F. Boyce, T. H. Williamson, H. L. Cook, E. Mensah, S. Lal, and D. Usher, "Automated detection of diabetic retinopathy on digital fundus images", *Diabet Med*, vol. 19, no. 2, pp.105-112, 2002.
7. D. Usher, M. Dumskyj, M. Himaga, TH. Williamson, S. Nussey, J. Boyce. "Automated detection of diabetic retinopathy in digital retinal images: a tool for diabetic retinopathy screening", *Diabet Med*, vol. 21, no. 1, pp.84-90, 2004.
8. G.G. Gardner, D. Keating, T.H. Williamson, A.T. Elliott, "Automatic detection of diabetic retinopathy using an artificial neural network: a screening tool", *Br J Ophthalmol*, vol. 80, no. 11, pp.940-944, 1996.
9. Z. Liu, C. Opas, and S.M. Krishnan, "Automatic image analysis of fundus photograph.", In *Engineering in Medicine and Biology Society, Proceedings of the 19th Annual International Conference of the IEEE 1997*, pp. 524-525.
10. A. Osareh, M. Mirmehdi, B. Thomas, R. Markham, "Automated identification of diabetic retinal exudates in digital colour images", *Br J Ophthalmol*, vol. 87, no. 10, pp.1220-1223, 2003.
11. S.K. Mitra, T.W. Lee, and M. Goldbaum, "A Bayesian network based sequential inference for diagnosis of diseases from retinal images.", *Pattern Recognition Lett*, vol. 26, no. 4, pp.459-470, 2005.
12. T. Kauppi, V. Kalesnykiene, J.K. Kamarainen, L. Lensu, I. Sorri, H. Uusitalo, H. Kälviäinen, and J. Pietilä, "DIARETDB0: Evaluation database and methodology for diabetic retinopathy algorithms", *Machine Vision and Pattern Recognition Research Group, Lappeenranta University of Technology, Finland*, 73, 2006.
13. STARE Project Website. Clemson, SC, Clemson Univ. [Online]. Available: <http://www.ces.clemson.edu/~ahoover/stare/>
14. R.C. Gonzales, R.E. Woods, "Digital image processing", New York: Addison-Wesley; 1993. p. 75-140.
15. A. Sopharak, B. Uyyanonvara, S. Barman, T.H. Williamson, "Automatic detection of diabetic retinopathy exudates from non-dilated retinal images using mathematical morphology methods", *Comput Med Imaging Graph*, vol. 32, no. 8, pp.720-727, 2008.
16. T. Walter, J.C. Klein, P. Massin, A. Erginay, "A contribution of image processing to the diagnosis of diabetic retinopathy-detection of exudates in color fundus images of the human retina.", *IEEE Trans Med Imaging*, vol. 21, no. 10, pp.1236-1243, 2002.
17. C.I. Sánchez, R. Hornero, M.I. Lopez, and J. Poza, "Retinal image analysis to detect and quantify lesions associated with diabetic retinopathy", *Engineering in Medicine and Biology Society, IEMBS'04. 26th Annual International Conference of the IEEE*, 2004, pp. 1624-1627.
18. Z. Xiaohui, and A. Chutatape, "Detection and classification of bright lesions in color fundus images", In *Image Processing*,

2004. ICIP'04. 2004 International Conference on IEEE, 2004, pp. 139-142.
19. A.K. Jain, "Fundamentals of digital image processing", Prentice-Hall, Inc., 1989.
 20. S. Badsha, A.W. Reza, K.G. Tan, K. Dimyati, "A new blood vessel extraction technique using edge enhancement and object classification.", J Digit Imaging, vol. 26, no. 6, pp.1107-1115, 2013.
 21. R. Akhavan, and K. Faez , "A novel retinal blood vessel segmentation algorithm using fuzzy segmentation", IJECE, vol. 4, no. 4, pp.561-572, 2014.
 22. M. García, C.I. Sánchez, M.I. López, D. Abásolo, R. Hornero, "Neural network-based detection of hard exudates in retinal images.", Comput Methods Programs Biomed, vol. 93, no. 1, pp.9-19, 2009.



Sara S. Aldeeb is currently a researcher at the Dept. of Computer Engineering in Istanbul University. She received her M.Sc. in 2017. Her main interests are Pattern Recognition, Artificial Intelligence and Image Processing



Selçuk Sevgen is currently an Assistant Professor at the Dept. of Computer Engineering in Istanbul University. He received his M.Sc. and Ph.D. degrees at the same department in 2003 and in 2009, respectively. His main interests are Neural Networks, CNNs